



# OBSERVATIONS OF STRESS AND LAMINATE THICKNESS VARIATIONS IN LCM PROCESSES

Simon Bickerton, William A. Walbran, Quentin Govignon [Simon Bickerton]:  
s.bickerton@auckland.ac.nz

Centre for Advanced Composite Materials, Department of Mechanical Engineering,  
The University of Auckland, Private Bag 92019, Auckland 1142, New Zealand

**Keywords:** tooling forces, laminate thickness, RTM, ICM, Resin Infusion

## Abstract

*Closed moulding processes are increasingly being used for the manufacture of fibre reinforced thermosets. A variety of mould construction methods and filling techniques are used, producing an ever expanding list of processes within the Liquid Composite Moulding (LCM) family. The long term goal of this research programme is the development of a generic LCM filling simulation, able to address processes utilising rigid, semi-rigid, and flexible moulds. This paper highlights recent developments in the experimental verification programme. A Tekscan dynamic pressure measurement system has been used to measure normal stresses exerted on a rigid mould during RTM and ICM cycles. A stereophotogrammetry technique has been employed to measure full field laminate thickness variations during Resin Infusion. Discussion is provided on initial results obtained with these systems.*

## 1 Introduction

The term Liquid Composite Moulding (LCM) encompasses a growing list of composite manufacturing processes. The vast majority of research has been completed on Resin Transfer Moulding (RTM), for which the moulds are assumed to be completely rigid. The range of LCM processes used in industry has increased, motivated by cost reduction and decreases in styrene emissions. The Injection/Compression Moulding (ICM) process offers reduction in cycle time, while LightRTM has been developed for lower cost semi-rigid moulds. By extending this concept further to totally flexible upper mould halves we have Resin Infusion (a.k.a. Vacuum Assisted RTM), which is being used to manufacture very large structures such as boat hulls and wind turbine blades. A major goal of this

research programme is the development of a generic LCM filling simulation.

This paper focuses on the detailed observations made on two experimental studies. For rigid mould processes such as RTM and ICM, a normal stress distribution is exerted on the mould. Tekscan, a distributed pressure measurement system provides significant insight to these complex stress patterns. For the Resin Infusion process a constant exterior pressure is exerted on the laminate, and dynamic thickness variations occur. A speckle stereophotogrammetry system has been developed, providing full field thickness measurements.

## 2 Rigid Tool Processes (RTM, ICM)

### 2.1 Motivation

Rigid tools dictate the laminate thickness distribution, resulting in a complex stress field being exerted on the mould surfaces. This normal stress is made up of components due to the fibre reinforcement's resistance to compaction, and to the resin pressure generated internally [1-3]. Accurate prediction of this stress field will improve modeling of LCM processes, allowing consideration of semi-rigid tooling used in processes such as LightRTM.

### 2.2 Experimental Facility

The Tekscan system provides dynamic measurements of pressure distribution at rates up to 8.0 Hz. In this study 238mm square sensors having a grid of 44 by 44 sensels were used. Two sensors were employed, with pressure ranges of 0-200 kPa and 0-1303 kPa. The pressure sensor is laid up between rigid aluminium plates, which are mounted in an Instron testing machine, as shown in Fig. 1. The upper mould plate is mounted using a spherical cross head mounting to eliminate misalignment of the mould platens. Both RTM and ICM cycles have been executed in this mould, the Instron providing

accurate control of mould platen position, and measurement of the total clamping force. Fig. 2 depicts one of the Tekscan sensors, alongside a 200 mm diameter sample of the glass fibre Chopped Strand Mat (CSM) used in this study.



Fig. 1. Experimental facility, aluminium platens mounted in Instron frame with TekScan sensor.

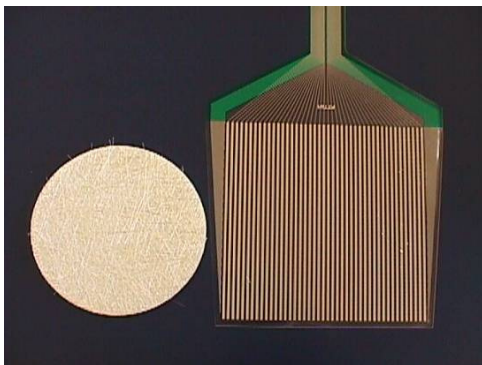


Fig. 2. CSM sample and Tekscan sensor.

## 2.3 Experimental Procedure

### 2.3.1 RTM

For the RTM experiments the preform and sensor were inserted and the mould then closed at a constant rate ( $\dot{h}_1$ ). When the target volume fraction ( $V_f$ ) was achieved, the Instron held the cavity

thickness ( $h_f$ ) constant while the fluid was injected at a constant pressure. Once full wet out of the fibre was achieved, the injection gate was closed.

### 2.3.2 ICM

As with RTM, the ICM process begins with the insertion of the preform into the mould cavity. The mould was then closed to an initial thickness ( $h_i$ ) greater than the final part thickness ( $h_f$ ), and a measured volume of fluid injected. Once sufficient resin was injected, the injection gate was closed. The mould cavity was then reduced to the desired part thickness at a constant speed ( $\dot{h}_2$ ), and hence fibre volume fraction.

An initial series of experiments was undertaken, the parameters of each given in Table 1. The test fluid in all cases was Mobil DTE AA mineral oil (viscosity 1.16 Pa.s at 20°C), and the injection pressure was a constant 200kPa. The resin was fed from a pressure pot, and the mass of resin injected during ICM experiments monitored using electronic weigh-scales. 10 layers of 450 g/m<sup>2</sup> chopped strand mat were used in all cases, the cavity thickness being adjusted to control the fibre volume fraction. Sample diameter is 200mm, with a 10mm diameter hole in the centre to enforce 2D flow.

Table 1. Experimental parameters

	$V_f$	$\dot{h}_1$ (mm/min)	$\dot{h}_2$ (mm/min)	$h_i$ (mm)	$h_f$ (mm)
RTM1	0.35	2	-	-	5
RTM2	0.50	2	-	-	3.2
ICM1	0.35	2	10	6	5
ICM2	0.50	2	10	6	3.2

## 2.4 Experimental Results

Fig. 3 shows the total force exerted on the mould surfaces for both RTM and ICM, low and high fibre volume fractions. The key phases of each process are indicated. As can be seen, the maximum force experienced during ICM (16.6kN for 0.50  $V_f$ ) is much greater than that experienced during RTM (6.1kN). This is due to the high secondary compaction speed during ICM, which results in a faster process, but at the cost of higher mould stresses, but at the cost of higher mould stresses. Fig. 3 shows this quite clearly, with the time to end of filling for ICM being 70s and 104s for the high and low volume fraction cases respectively, compared to 1166s and 475s during RTM. The total mould forces as recorded by the TekScan sensors

compare favourably with both analytical solutions, and load cell data previously recorded [2, 4].

2.4.1 RTM

Shown in Fig. 4 are pressure distributions recorded at three major stages of the process for both low and high volume fractions; a) just prior to injection of fluid at the completion of the compaction phase, b) at the completion of the filling phase, and c) at the end of the process indicating the steady state compaction response.

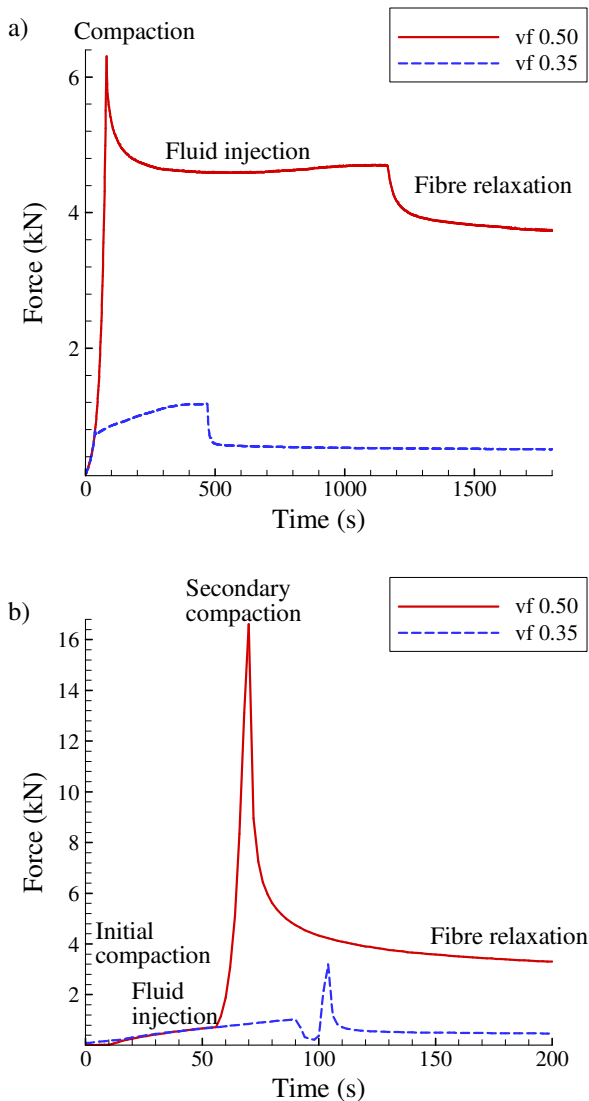


Fig. 3. Total force traces during a) RTM and b) ICM.

It is clear from the stress fluctuations in Fig. 4 that the CSM is quite un-homogeneous, despite it's relatively homogeneous physical appearance, even with 10 layers of mat being compacted. However, we can see that the average compaction response

across the mould in Fig. 4a and 4d is relatively uniform as would be expected [5,6].

For the low fibre volume fraction case, it is clear from Fig. 4b that the total stress observed during the process is significantly influenced by the fluid pressure, as moderate compaction is required to compress the fibre to the desired volume fraction (0.35). However, in the case of higher fibre volume fraction (0.50), the fibre stress is very dominant. In this case, the fluid pressure has little impact on the total stress, as shown in Fig. 4e, and in fact the maximum stress recorded for this case is after compaction (Fig. 4d). This would indicate that the stress relaxation that is occurring does so at a greater rate than the fluid pressure increases the total stress. This observation is reinforced by Fig 3a where we can see that for the high volume fraction case, the maximum force exerted on the mould is at the end of the compaction phase, and drops away during the injection phases. However, the low volume fraction experiment recorded the maximum force at the completion of the filling phase. In both cases, after the fluid has been injected and the inlet gate closed, the fluid pressure drops to zero leaving only the fibre stress which continues to relax to a steady state (Fig. 4c and 4f).

2.4.2 ICM

Fig. 5 depicts similar pressure distributions for the ICM experiments. Again, both low and high volume fraction experiments are shown at key phases of the process. In this instance, the key phases are; a) completion of initial compaction, prior to filling, b) completion of filling, c) completion of second compaction phase to final volume fraction, and d) at the end of the process indicating the steady state compaction response. It should be noted that for the high volume fraction ICM experiment, the higher range sensor was used as the low range sensor reached saturation very early in the process. As a result, the initial compaction phase of the experiment resulted in very few sensels being excited beyond their threshold. This is demonstrated by comparing Fig. 5a, where the entire sample area is being excited, with Fig. 5e, where only a small number of sensels are being excited. In both cases the samples are loaded to the same approximate cavity thickness, and hence total stress as measured by the Instron load cell.

As with RTM, in the low volume fraction process case the fluid pressure is much more prominent than the fibre compaction stress. At the completion of the filling stage (Fig. 5b), the fluid

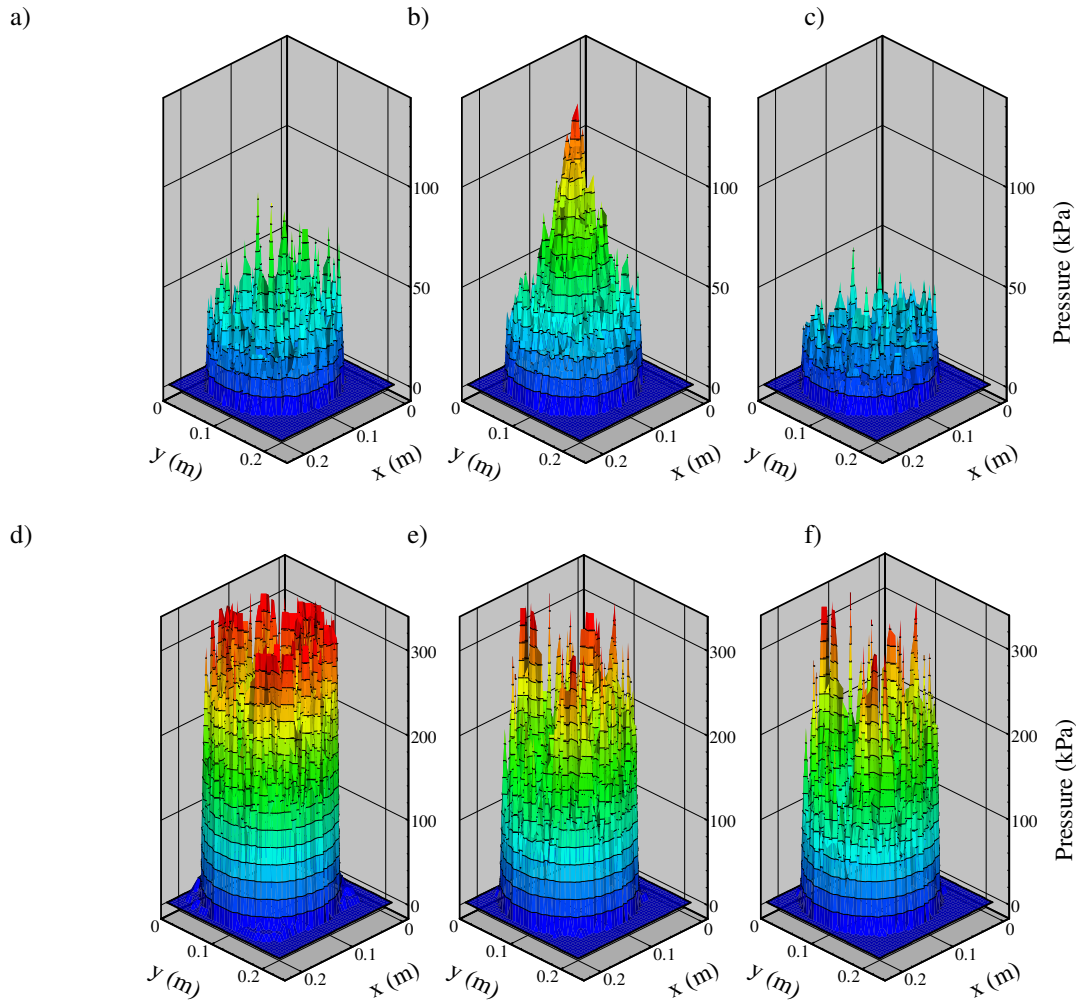


Fig. 4. Pressure distributions at key phases during RTM of CSM. a)  $V_f = 0.35$  and d)  $V_f = 0.50$  After compaction, prior to filling, b)  $V_f = 0.35$  and e)  $V_f = 0.50$  the end of the injection phase, and c)  $V_f = 0.35$  and f)  $V_f = 0.50$  steady state compaction response.

pressure field completely dominates the compaction stress. After the second compaction phase (Fig. 5c), the fibre compaction stress has increased, however the total stress is still dominated by the fluid pressure field as the fluid has been driven through the reinforcement. It is interesting to note the difference in irregularity at the end of the filling phase (Fig. 5b) and the end of the second compaction phase (Fig. 5c). This shows the increased influence of fibre compaction stress as the preform is compressed further, though fluid pressure is still dominant. It is also interesting to note the shape of the measured fluid pressure distributions, comparing well to the logarithmic analytical solution during injection, and to the parabolic solution predicted during compression flows [2].

The high volume fraction ICM case is somewhat different. Fig. 5f highlights the low fluid

pressures at the completion of filling as compared to the maximum stress, which is experienced at the completion of the second compaction phase (Fig. 5g). As with RTM, the higher fibre compaction stress contributes towards the total stress more significantly than for the low volume fraction case. However, the majority of the total stress is due to fluid pressure at the completion of the compression flow phase. This observation is confirmed by the large drop in total force at the completion of filling (Fig. 3b).

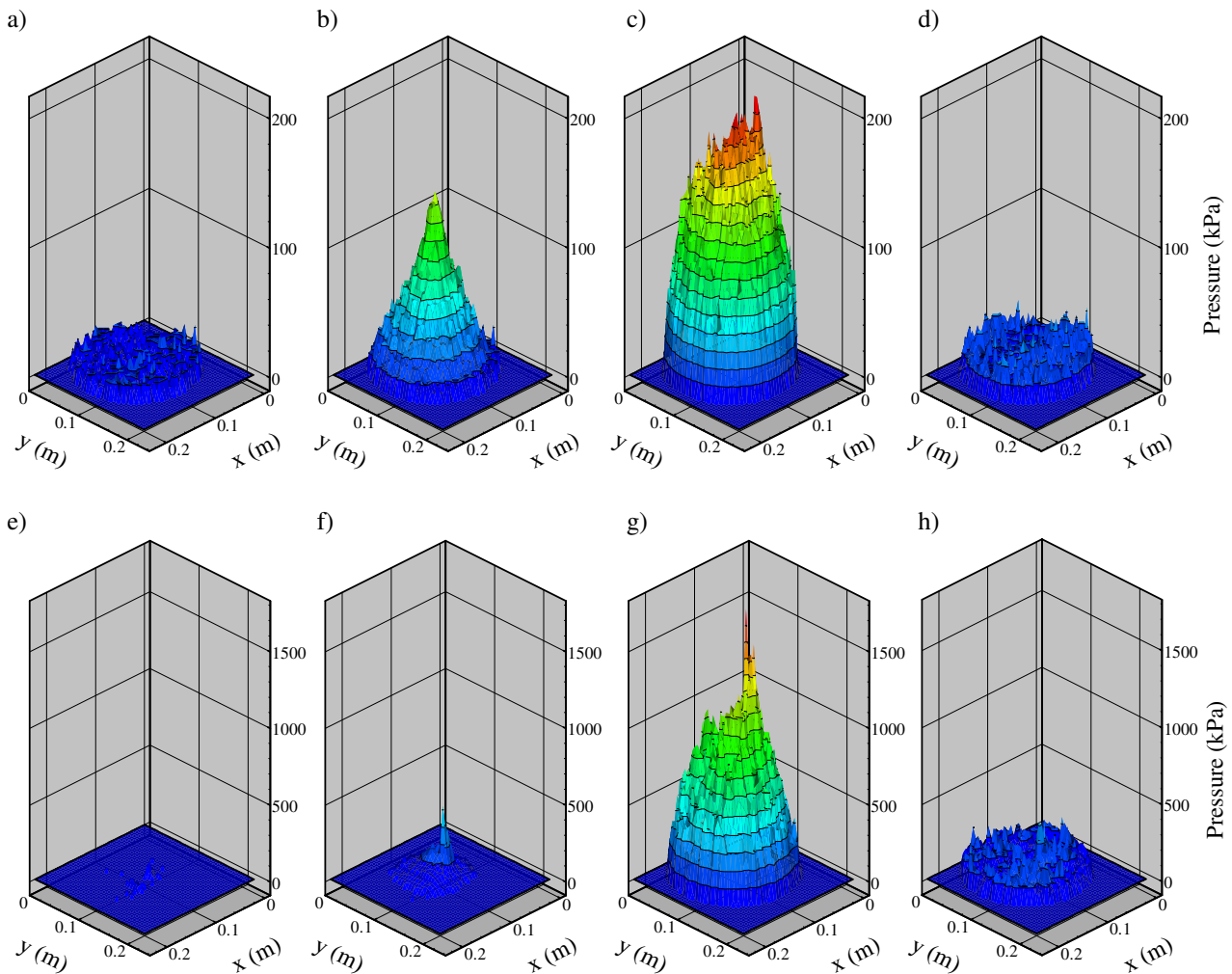


Fig. 5. Pressure distributions at key phases during ICM of CSM. a)  $V_f = 0.35$  and e)  $V_f = 0.50$  After initial compaction, prior to filling, b)  $V_f = 0.35$  and f)  $V_f = 0.50$  after fluid has been injected, c)  $V_f = 0.35$  and g)  $V_f = 0.50$  at the end of the second compaction phase, and d)  $V_f = 0.35$  and h)  $V_f = 0.50$  steady state compaction response.

### 3 Soft Tool Processes (Resin Infusion, VARTM)

#### 3.1 Motivation

In the Resin Infusion and other soft tool LCM processes, laminate consolidation is due to the pressure applied to the flexible side of the mould. Compaction of the fibre reinforcement results from the balance between external atmospheric pressure and the internal resin pressure, following Terzaghi's relation. Due to the complex compaction behaviour of the fibrous reinforcement and the dynamic variation of the internal resin pressure, the laminate thickness evolves prior to, during, and after the filling stage of Resin Infusion. These changes in laminate thickness have the potential to significantly affect local permeability of the reinforcement. The

ability to model these thickness changes is therefore important for accurate simulation of this process.

#### 3.2 Experimental Facility

The experimental Resin Infusion facility at the University of Auckland allows for measurement of resin pressures within the laminate, resin flow rates, and laminate thickness. The infusion table is also temperature controlled, allowing control of resin viscosity. Previous point measurements of laminate thickness have produced erratic results, motivating the development of full field measurements. A stereophotogrammetry system has been developed, allowing thickness measurements across the full surface of a laminate to a resolution of 0.01 mm. From this thickness data, detailed full field information is available on fibre volume fraction and

permeability. Fig. 6 presents the experimental setup, including the temperature controlled table, and the stereophotogrammetry system.



Fig. 6. Experimental Resin Infusion facility.

### 3.2.1 Temperature Controlled Table

The mould used in the experimental programme is a sandwich structure of 50 mm foam core, bounded by 3 and 5 mm aluminium plates. The temperature is controlled via a water track running under the top plate. The water track is connected to a heat exchanger and the temperature of the mould is monitored by a series of thermocouples. Three ports have been installed along the mould to mount pressure transducers, which are used to monitor the internal resin pressure.

### 3.2.2 Stereophotogrammetry System

The stereophotogrammetry system employs two high resolution digital cameras, taking pictures of the entire laminate from two slightly different angles. In this way a complete thickness map of the laminate can be captured at a particular instant. The cameras are mounted on a frame 1.8 m above the table, separated by a horizontal distance of 1.1 m. The technique applied in this study uses two verging axis cameras, but the displacement is measured on pictures from the same camera. The vacuum bag is painted with a high frequency pattern (Fig. 7) to enable matching of the pictures via software. The processing of the images is done using a program developed for this purpose by the Communication and Information Technology Research centre (CITR) from the University of Auckland (see [7] for more details).

### 3.2.3 Data Acquisition System

Acquisition of the experimental data is made using two systems. The thickness data are extracted from the stereophotogrammetry system, photographs being captured by the cameras at regular intervals during an experiment. A very large amount of data is recorded for each experiment, which requires a significant amount of post-processing to extract the thickness field. The remaining acquisitions are local measurements, and the data is recorded during processing using LabView. The resin flow rate into the laminate is measured at the inlet by weighing the resin pot. Three pressure transducers embedded in the mould along the length of the preform measure the resin pressure inside the laminate, and the vacuum pot pressure is also recorded. Along with data acquisition, the LabView interface is responsible for controlling the temperature of the mould via the heat exchanger, and for controlling the timing of the image acquisition.



Fig. 7. High frequency pattern on the vacuum bag.

## 3.3 Sample Experimental Data

An extensive experimental programme is in progress, and the evolution of laminate thickness, resin pressures, and resin flow rates will be monitored. This data is required to better understand Resin Infusion, and for comparison to simulations under development. A single experiment is presented in detail in this paper.

### 3.3.1 Materials and Procedures

The experiment described here was performed using a glass fibre stitched biaxial fabric (800g/m<sup>2</sup>). The test fluid used here is the Mobil DTE AA mineral oil, chosen as it has a viscosity similar to that of a Resin Infusion grade resin at the working temperature. Nine plies of 850 by 250 mm were laid

up on the table in the same orientation to form the laminate  $[0-90]_9$  (Fig. 8). A single layer of peel ply and distribution medium were laid over the laminate. The mould was then sealed with a vacuum bag. Once sealed both the laminate and the test fluid are left on the table while the temperature equalises to  $30^\circ\text{C}$ . Vacuum is applied after equilibration of the temperature. Once the laminate is fully evacuated, the inlet is then opened. The inlet is clamped once the resin reaches the end of the preform. The vent remains open at full vacuum during both the filling and post-filling phases.

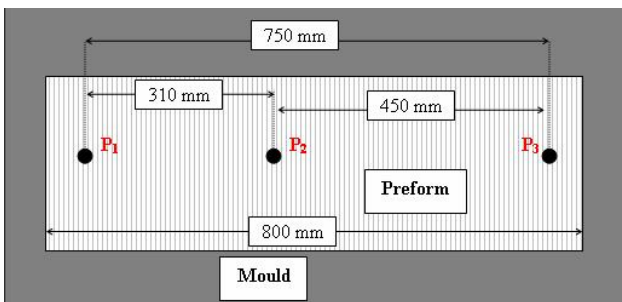


Fig. 8. Layout of the preform and pressure transducers.

### 3.3.2 Results

Presented in Fig. 9 are laminate thickness maps recorded at key stages during the experiment. In each frame the inlet is at the left, and the vent the right side of the images. Fig. 9a is the map at the beginning of the filling,  $Del$  representing the change in the thickness from the value at the completion of evacuation. Fig. 9b was captured midway through the filling phase, Fig. 9c at the completion of filling, and Fig. 9d at the end of the post-filling period.

A small drop in thickness can be noted just lagging the flow front. This effect is caused by the lubricating effect of the fluid on the fibrous reinforcement. The thickness increase behind the flow front on the inlet side is due to the increase in resin pressure. This results in a lower compaction stress being applied to the reinforcement. During the post-filling period the laminate thickness decreases. The largest reduction is noted at the inlet, where the greatest changes in resin pressure are expected. It should be noted that the post-filling phase represents a similar time period as for filling, the process of drawing any excess resin through the length of the mould being very slow.

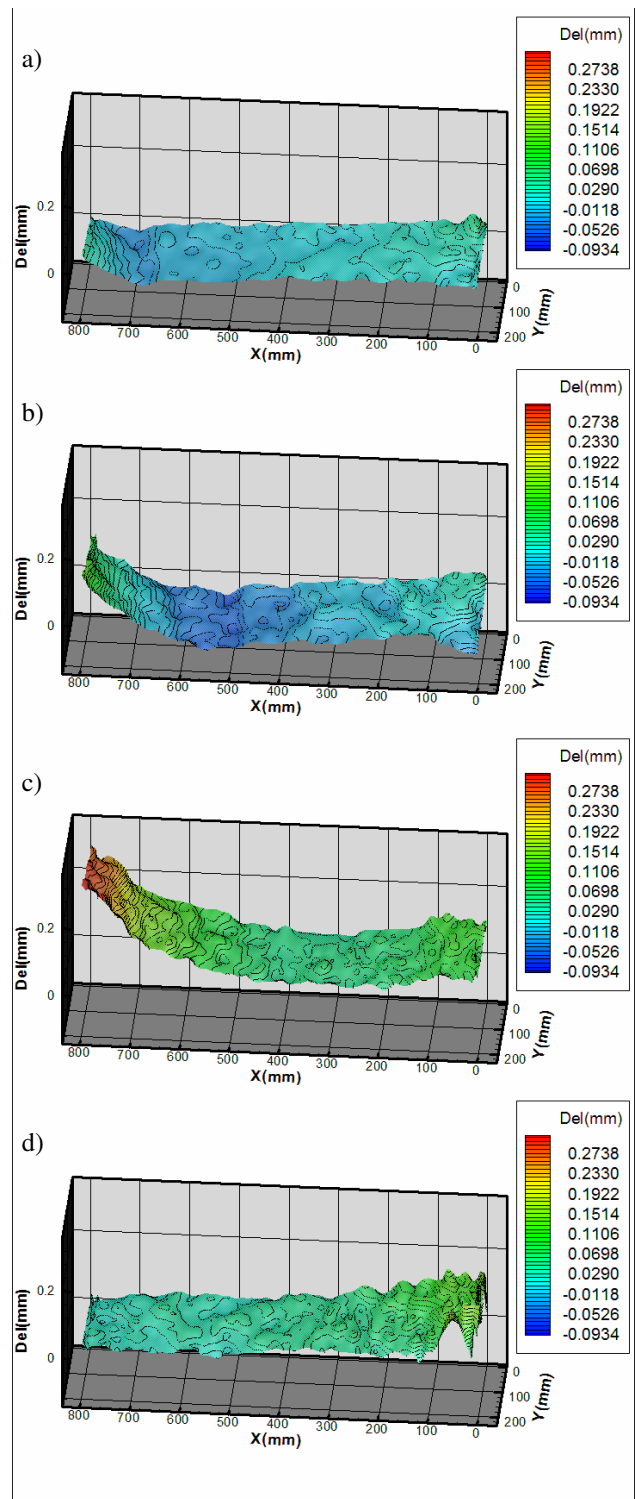


Fig. 9. Maps of thickness variation at different times during the experiment. a) 210 s into the infusion, b) 530 s after the start of the infusion, c) at  $t=1490$  s, just before clamping the inlet, and d) at the end of the post-filling phase.

In Fig. 10a the resin pressure in the laminate is compared to the local thickness at those points. Fig. 10b presents the resin flow rate at the inlet. The variation of thickness in the laminate can be related to the resin pressure inside the laminate, but there is a clear viscoelastic effect. Near the inlet, the resin pressure builds up very quickly and reaches a plateau around 900 mbar, while the laminate thickness in this area increases steadily during the

same period. The same can be noted around the middle of the laminate and the outlet.

The fibre volume fraction can be calculated from the thickness using the following equation;

$$V_f = \frac{N \cdot W}{\rho_f \cdot h} \quad (1)$$

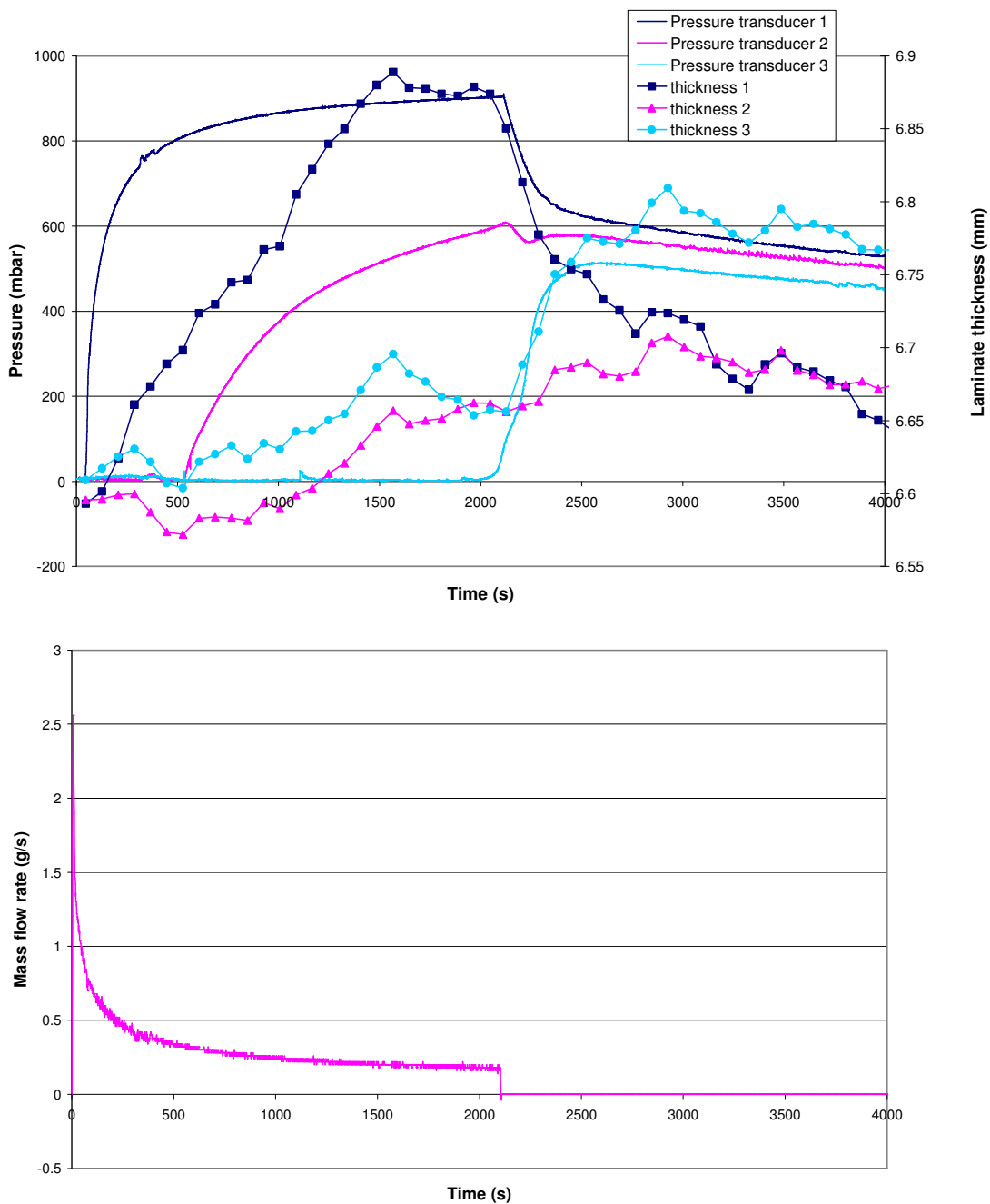


Fig. 10. a) Evolution of fluid pressure and laminate thickness at three points in the mould. b) Evolution of fluid flow rate at the inlet.

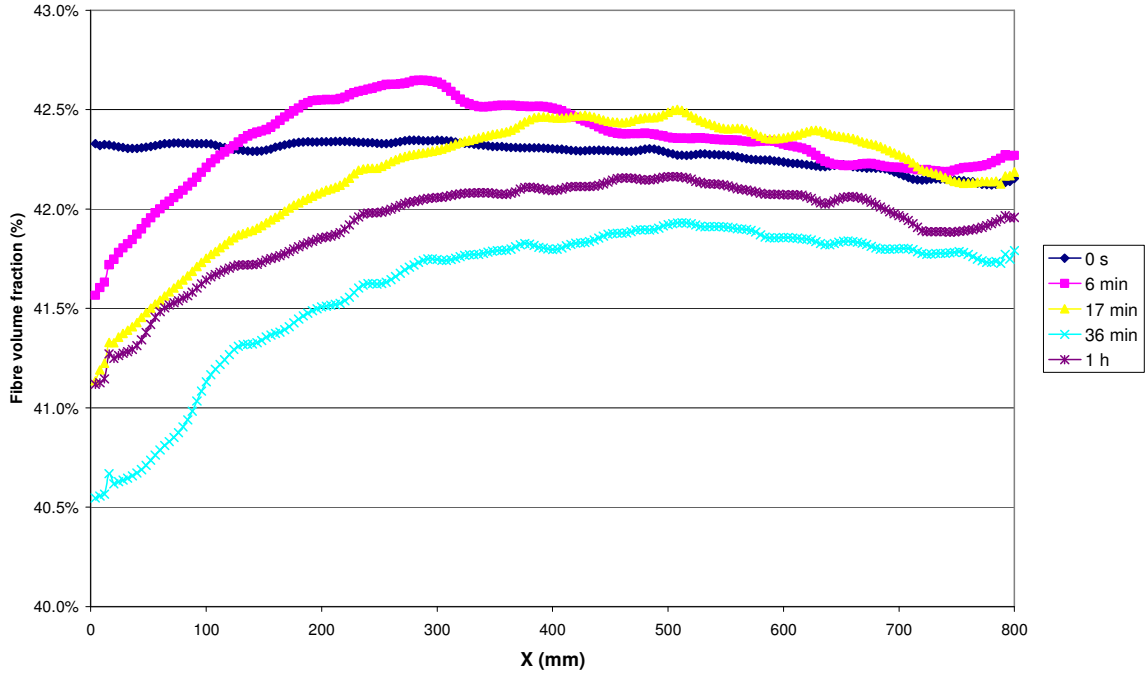


Fig. 11. Calculated  $V_f$  variation along the preform length at several instances during the experiment.

where  $N$  is the number of layers in the preform,  $W$  is the mass of the reinforcing fabric per unit area (in  $\text{kg/m}^2$ ),  $\rho_f$  is the density of the fibre material, and  $h$  is the measured thickness of the laminate at any instant. Fig. 11 presents volume fractions calculated along the length of the laminate at several instances. This data is calculated from a sample taken along the laminate centreline. The laminate  $V_f$  varies most strongly around the inlet, and although these variations can appear quite limited they greatly affect the permeability of the reinforcement, and the flow of the resin. The variation of thickness and permeability has proven even more dramatic for laminates without distribution media, or laminates using a highly permeable continuous filament mat for resin distribution [8].

### 3.3.3 Discussion

The reinforcement permeability is strongly dependant on the fibre volume fraction. Models such as the Carman-Kozeny equation can be used to link the permeability to the  $V_f$  as follows:

$$K = \frac{d^2}{16 \cdot k} \cdot \frac{(1 - V_f)^3}{V_f^2} \quad (2)$$

where  $d$  is the fibre diameter and  $k$  is the dimensionless Kozeny constant found from experiment. Small variations in the thickness of the laminate during the Resin Infusion process will

therefore influence the permeability of the preform, and thus affect the dynamic of the filling and post-filling processes. The stereophotogrammetry system introduced in this paper will provide a better understanding of such behaviour, and will be used to explore the influence of various laminate constructions, and filling conditions. This tool may also be further developed for control applications, being of use to decide when and how to change the pressure conditions at the inlets and vents, in order to minimize the length of the post-filling phase, and improve the uniformity of laminate quality.

## 4 Conclusions

As LCM processes are employed more widely, an increasing number of process variants are being developed. Application of injection and compression driven flows within flexible and semi-rigid moulds provides a range of manufacturing opportunities, while introducing significant challenges for mould and process design. The Tekscan distributed pressure measurement system has been used in this study to explore the complex, dynamic stress distributions exerted on rigid tools during RTM and ICM. The initial experiments have highlighted significant fluctuations in fibre compaction stress generated by a glass fibre random mat, though the fibre volume fraction remained constant in the mould. The relative influence of compaction stress

and fluid pressure has been demonstrated, which will be defined by the permeability and compaction response of the fibre reinforcement applied. The fluid pressure fields observed compare qualitatively well with analytical solutions, providing confidence governing equations applied for simulation. Application of the Tekscan system will be expanded to a more detailed RTM and ICM study, and to investigate the spatial homogeneity of fibre compaction stress for a selection of common LCM reinforcements.

An experimental Resin Infusion setup has been established around a large temperature controlled mould. A stereophotogrammetry system provides full field thickness maps at a spatial resolution of 0.01 mm, to a rate of one frame every five seconds. This extensive thickness data is supplemented by point measurements of fluid pressure at three points, and a continuous measurement of the fluid flow rate at the inlet. The presented example experiment has highlighted small, but significant thickness variations during the filling and post-filling phases. The potential for such thickness variations to influence mould filling and final part quality will depend strongly on the flow resistance and compaction response of the laminate. A more extensive study will be completed, considering the influence of distribution media, various reinforcement styles, and different processing conditions.

## 5 References

- [1] Han K., Ni J., Toth J., Lee L.J. and Green J.P. "Analysis of an injection/compression liquid composite molding process". *Polymer Composites*, Vol. 19, No. 4, pp 487-496, 1998.
- [2] Bickerton S. and Buntain M.J. "Modeling forces generated within rigid liquid composite molding tools; part B numerical analysis". *accepted to Composites Part A*, 2007.
- [3] Deleglise M., Binetruy C. and Krawczak P. "Simulation of LCM processes involving induced or forced deformations". *Composites Part A*, Vol. 37, No. 6, pp 874-880, 2006.
- [4] Buntain M.J. and Bickerton S. "Modeling forces generated within rigid liquid composite molding tools; part A experimental study". *accepted to Composites Part A*, 2007.
- [5] Pearce N. and Summerscales J. "The compressibility of a reinforcement fabric". *Composites Manufacturing*, Vol. 6, No. 1, pp 15-21, 1995.
- [6] Bickerton S., Buntain M.J. and Somashekar A.A. "The viscoelastic compression behavior of liquid composite molding preforms". *Composites Part A*, Vol. 34, No. 5, pp 431-444, 2003.
- [7] Lin Y., Morris J., Govignon Q. and Bickerton S. "Digital speckle photogrammetry". *Proceedings of the 21st International Conference Image and Vision Computing New Zealand*, Great Barrier Island, New Zealand, 2006.
- [8] Govignon Q., Bickerton S., Morris J. and Lin J. "A stereo photography system for monitoring full field thickness variation during resin infusion". *Proceedings of the 8th International Conference on Flow Processes in Composite Materials*, Douai, France, pp 231-239, 2006.